Drug Delivery

DOI: 10.1002/ange.201207721

On-Demand Drug Release System for In Vivo Cancer Treatment through Self-Assembled Magnetic Nanoparticles**

Jae-Hyun Lee, Kuan-Ju Chen, Seung-Hyun Noh, Mitch André Garcia, Hao Wang, Wei-Yu Lin, Heeyeong Jeong, Brian Junoh Kong, David B. Stout, Jinwoo Cheon, and Hsian-Rong Tseng**

The intrinsic nature of small-molecule chemotherapeutics, including 1) limited aqueous solubility, 2) systemic toxicity because of a nonspecific whole-body distribution, and 3) potential development of drug resistance after initial administration, compromises their treatment efficacy.[1] Recently, nanoparticle (NP)-based drug delivery systems have been considered as promising alternatives to overcome some of these limitations and begin to resolve obstacles in the disease management in clinical oncology.[2] The intraparticular space of a NP vector can be employed to package drug payloads without constrain associated with their solubility. Further, NP vectors exhibit enhanced permeability and retention (EPR) effects[3] that facilitate the differential uptake, leading to a preferential spatio-distribution in the tumor.[4] However, conventional NP drug delivery systems tend to passively release drug payloads, limiting the ability to release an effective drug concentration at a desired time window. Therefore, there is a need to develop next-generation NP drug delivery system such as a stimuli-responsive drug release system with the goal of achieving spatio-temporal control, by which an acute level of drug concentration can be delivered at the time point when the NP vectors reach maximum tumor accumulation.[5] By doing so, it is expected to dramatically improve therapeutic effects in the tumor and effectively reduce systematic toxicity at a minute drug dosage.[6]

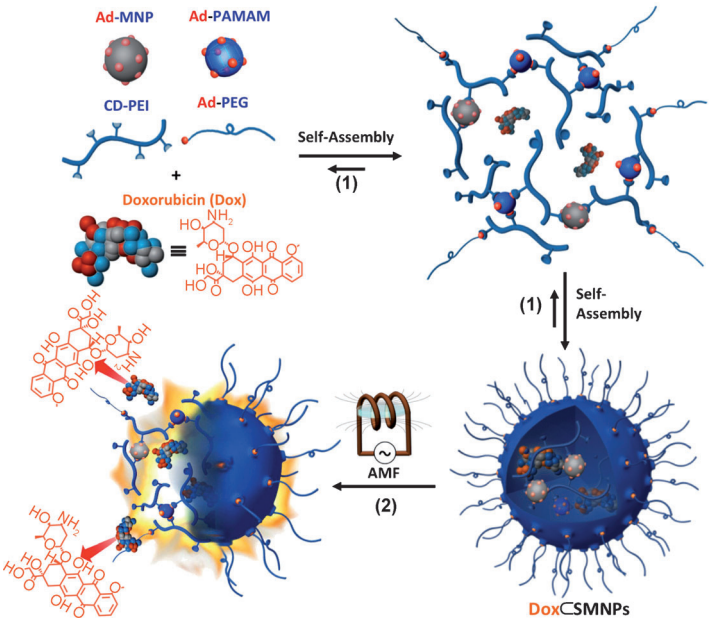

Scheme 1. Molecular design, self-assembly, and function of magnetothermally responsive doxorubicin (Dox)-encapsulated supramolecular magnetic nanoparticles (DoxCSMNPs). 1) The self-assembled synthetic strategy is employed for the preparation of DoxCSMNPs, which is made from a fluorescent anticancer drug (Dox) and four molecular building blocks: Ad-PAMAM, 6 nm Ad-grafted $Zn_{0.4}Fe_{2.6}O_4$ superparamagnetic nanoparticle (Ad-MNP), CD-PEI, and Ad-PEG. 2) The embedded Ad-MNP serves as a built-in heat transformer that triggers the burst release of Dox molecules from the magnetothermally responsive SMNP vector, achieving on-demand drug release upon the remote application of an alternative magnetic field (AMF).

Previously, we demonstrated a convenient, flexible, and modular self-assembled synthetic approach for the preparation of supramolecular nanoparticle (SNP) vectors from a collection of molecular building blocks through a multivalent molecular recognition between adamantane (Ad) and β-cyclodextrin (CD) motifs.[7] Such a self-assembled synthetic strategy enables control over the sizes, surface chemistry, and payloads of SNP vectors for a wide

[*] Dr. J.-H. Lee,[+] S.-H. Noh, H. Jeong, Prof. J. Cheon
Department of Chemistry, Yonsei University
Seoul 120-749 (Korea)
E-mail: jcheon@yonsei.ac.kr
Dr. K.-J. Chen,[+] Dr. M. A. Garcia,[+] Prof. H. Wang, Prof. W.-Y. Lin, B. J. Kong, Prof. D. B. Stout, Prof. H.-R. Tseng
Department of Molecular and Medical Pharmacology
Crump Institute for Molecular Imaging (CIMI)
California NanoSystems Institute (CNSI)
Institute for Molecular Medicine (IMED)
University of California, Los Angeles
Los Angeles, CA 90095-1770 (USA)
E-mail: hrtseng@mednet.ucla.edu
Homepage: http://tseng-lab.com
Prof. H. Wang
National Center for Nanoscience and Technology
11 Beiyitiao Zhongguancun Haidian District
Beijing, 100190 (P.R. China)
Prof. W.-Y. Lin
Department of Medicinal and Applied Chemistry
Kaohsiung Medical University
100, Shih-Chuan 1st Road, Kaohsiung, 80708 (Taiwan)
[+] These authors contributed equally to this work.

[**] This research was supported by the NIH (grant numbers R21GM098982 and R21EB016270; H.R.T.), National Creative Research Initiative (2010-0018286; J.C.), and WCU (R32-10217; J.C.).
Supporting information for this article is available on the WWW under http://dx.doi.org/10.1002/anie.201207721.

range of diagnostic and therapeutic applications such as positron emission tomography (PET) imaging,[7] magnetic resonance imaging (MRI),[8] photothermal treatment,[9] as well as highly efficient delivery of genes,[10] transcription factors,[11] and drug–polymer conjugates.[12]

Herein, we introduce magnetothermally responsive doxorubicin-encapsulated supramolecular magnetic nanoparticles (Dox⊂SMNPs) as a unique on-demand drug delivery/release system (Scheme 1). The supramolecular synthetic strategy[7–12] was employed to prepare size-controllable Dox⊂SMNPs composed of the fluorescent anti-cancer drug, Dox, and four different molecular building blocks, including Ad-grafted polyamidoamine dendrimers (Ad-PAMAM), β-CD-grafted branched polyethylenimine (CD-PEI), Ad-functionalized polyethylene glycol (Ad-PEG), and 6 nm Ad-grafted $Zn_{0.4}Fe_{2.6}O_4$ superparamagnetic nanoparticles (Ad-MNP). The EPR effects are expected to drive preferential tumor accumulation of Dox⊂SMNPs,[4,13] which constitutes the spatio-control of Dox⊂SMNPs. According to our design, the embedded magnetic NP (Ad-MNP) serves as a built-in transformer that converts radiofrequency external alternative magnetic field (AMF) into heat, allowing for stimuli-responsive drug release from Dox⊂SMNPs. To determine the ideal size of Dox⊂SMNPs for the proper spatial distribution and optimal temporal point for the maximized tumor accumulation of Dox⊂SMNPs, ^{64}Cu-labeled Dox⊂SMNPs are prepared by incorporating a radioisotope (i.e., $^{64}Cu^{2+}$) in the presence of a DOTA ligand (DOTA = 1,4,7,10-tetraazacyclododecane-1,4,7,10-tetraacetic acid) and then subjected to PET-based in vivo imaging studies. In parallel, the optimal AMF condition was determined by monitoring Dox release from Dox⊂SMNPs in vitro. Based on the results from both in vivo biodistribution and in vitro AMF optimization studies, we were able to design an optimized in vivo protocol for Dox⊂SMNPs to accomplish effective cancer therapy. Taken together, an acute level of drug concentration can be delivered to a tumor with spatiotemporal control thus significantly reducing the drug dosage.

The strong heat induction from zinc-doped MNP, because of its higher saturation magnetization value, makes this inorganic NP an ideal component for incorporation into our thermally responsive SNP vector.[14] We modified the 6 nm zinc-doped MNP with Ad, so that Ad-MNP (Figure 1 a) can serve as one of the molecular building blocks for incorporation into Dox⊂SMNPs through self-assembly. By fine-tuning the different ratios of the molecular building blocks, three sizes of Dox⊂SMNPs are prepared (70, 100, and 160 nm, Figure 1 b–d). All three sizes of the Dox⊂SMNPs have a narrow size distribution measured by light scattering, and the Dox encapsulation efficiency is determined to be about 95 % (see Figure S2 in the Supporting Information).

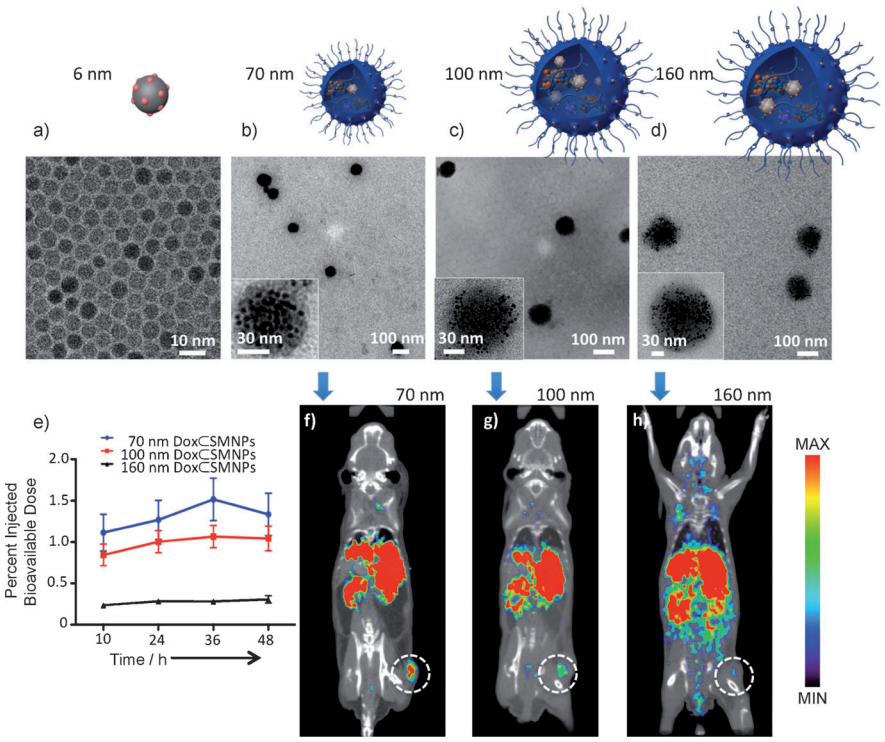

Figure 1. Characterization and biodistribution of Dox⊂SMNPs. a–d) Transmission electron microscope (TEM) images of a) 6 nm Ad-MNP and Dox⊂SMNPs with various sizes of b) 70 ± 9, c) 96 ± 7, and d) 161 ± 8 nm. Insets: Higher magnification TEM images of each Dox⊂SMNPs. e) Time-dependent accumulation of the three Dox⊂SMNPs in the tumor versus the whole body of NU/NU mice measured by micro-PET ($n = 3$). f–h) 2-D micro-PET cross-sections images, created using a filtered back-projection, of mice bearing a DLD-1 tumor ($n = 3$) at 36 h post-injection of 70, 100, and 160 nm ^{64}Cu-labeled Dox⊂SMNPs. Each image was scaled to its own maximum. The 70 nm Dox⊂SMNPs show the highest tumor-specific uptake among the three studies.

A key physical parameter that determines the overall biodistribution pattern and therapeutic performance is the size of the Dox⊂SMNPs.[2b,15] We used micro-PET imaging to identify an optimal size of the Dox⊂SMNPs with the highest retention in a tumor. Three sizes (70, 100, and 160 nm) of ^{64}Cu-labeled (300 μCi) Dox⊂SMNPs were synthesized (see the Supporting Information) and injected into DLD-1 tumor-bearing NU/NU mice by intravenous (i.v.) administration. The time-dependent accumulation of the three Dox⊂SMNPs in the tumor versus the whole body are summarized and plotted in Figure 1 e. The results show that the 70 nm Dox⊂SMNPs achieve their maximum tumor accumulation at 36 h post-injection, which is the critical time point for the optimal spatial distribution of Dox⊂SMNPs. The representative two-dimensional cross-sections of static filtered back-projection micro-PET images of the three Dox⊂SMNPs taken at 36 h post-injection are shown in Figure 1 f–h, indicating that 70 nm Dox⊂SMNPs have the highest tumor-specific uptake among the three sizes; therefore, the 70 nm Dox⊂SMNPs were chosen and used for further in vitro and

in vivo studies. We note that the high signal measured in the liver should not be a major concern since it is presumably due to demetalation of ^{64}Cu from the DOTA ligand,[16] and thus does not accurately represent the location of Dox⊂SMNPs in that organ (see quantified biodistribution and clearance data in the Supporting Information).

The self-assembly of Ad-PAMAM, Ad-MNP, CD-PEI, and Ad-PEG generates SMNP vectors with intraparticular cationic hydrogel networks. Such hydrogel networks constitute a unique nano-environment that induces self-organization of Dox molecules driven by their intermolecular π–π stacking interactions.[17] As a result, the fluorescent signal of encapsulated Dox molecules is quenched almost completely (ca. 97%, see Figure S3) when associated with the SMNP vector. AMF is used as an external on-demand control to trigger the fast release of encapsulated Dox from the disassembled SMNP vector through magnetic heating.[9] Once released from the SMNP vector, the fluorescence of Dox molecules is restored. We used this photophysical property of Dox to investigate the magnetically activated drug release performance of Dox⊂SMNPs as a function of the AMF duration (500 kHz, 37.4 kA m^{-1}). The results show that the drug release from Dox⊂SMNPs nearly saturates with 10 minutes of AMF without raising the temperature of the surrounding solution (see Figure S7b). When we applied multiple AMF pulses for a duration of 2 minutes to the Dox⊂SMNPs with an 8 minutes interval (Figure 2a), approximately 50% of the encapsulated Dox molecules are released in the first AMF pulse (Figure 2a, red line), while more Dox is released in a stepwise fashion after subsequent AMF pulses up to 7 or 8 pulses (50 minutes; Figure 2a, black line). Based on these results, we selected a single pulse of the AMF application with a 10 minutes duration as an effective AMF condition of Dox⊂SMNPs-based drug delivery system in further in vitro and in vivo studies, which can achieve on-demand release of an acute level of Dox concentration while avoiding unregulated drug release and thermal heating of the surrounding medium.

In vitro on-demand release of Dox from the 70 nm Dox⊂SMNPs were investigated for a DLD-1 colorectal adenocarcinoma cell line with (Figure 2b, left column) and without (Figure 2b, right column) the application of a 10 minutes AMF (500 kHz, 37.4 kA m^{-1}). After the cells (1.5×10^4) are treated with the 70 nm Dox⊂SMNPs (200 μg mL^{-1} treatment), minimal drug release with dim Dox fluorescence and no cell damage are observed (Figure 2b, right column). However, after exposure to AMF, blebbing and Dox fluorescence (red) is significantly increased (Figure 2b, left column). Also, nucleus fragmentations[18] and formation of apoptotic cell bodies are seen, demonstrating the consequence of effective Dox release from the Dox⊂SMNPs under AMF application. A CCK-8 assay is used to quantify the cell viability showing the decrease of the viability to 30% after AMF application. Without the application of AMF, negligible cytotoxicity is observed and AMF alone has no effect on the cell viability (Figure 2c).

Based on the systemic biodistribution results (optimal time point, i.e., 36 h post-injection, Figure 1e) and the in vitro drug release experiments (favorable AMF condition, i.e., 10 min, Figure 2), we designed an idealized in vivo treatment protocol of the 70 nm Dox⊂SMNPs for cancer therapy. When the tumor volume of DLD-1 xenografted mice ($n=3$) reached 100 mm^3, the Dox⊂SMNPs (70 nm, 150 μg kg^{-1}) were administered intravenously (day 0) followed by AMF treatment (10 minutes, 500 kHz, 37.3 kA m^{-1}) after 36 h post-injection. Anti-tumor efficacy results treated with Dox⊂SMNPs (w/and w/o AMF) and other control studies (i.e., AMF only and PBS only; PBS = phosphate buffered saline) are summarized as plots of tumor volume over the course of treatment in Figure 3a. The control groups (i.e., Dox⊂SMNPs w/o AMF, AMF only, and PBS) do not show any statistically significant differences in tumor suppression (Figure 3a). The group treated with a single injection of Dox⊂SMNPs with applied AMF shows tumor suppression efficacy only up to day 7 (Figure 3a, red line). In contrast, the group treated with a double injection (day 0 and day 7) of Dox⊂SMNPs with AMF shows continued and effective inhibition of tumor growth (Figure 3a, black line). The tumor images of each group are shown in Figure 3b, which visually confirm the effective tumor suppression of the doubly

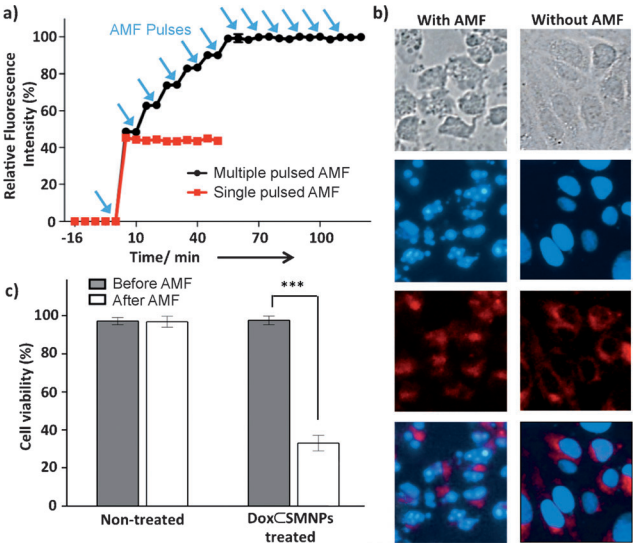

Figure 2. In vitro drug release and therapeutic efficacy of the 70 nm Dox⊂SMNPs. a) Dox release profiles upon the application of AMF in either multiple pulses (black line; 2 minutes of pulse duration with 8 minutes of non-pulsed intermittence) or in a single pulse (red line; 2 minutes of pulse duration). Approximately 50% of the encapsulated Dox molecules are released in the first AMF pulse and the rest of the Dox molecules is released stepwise in subsequent AMF pulses. Blue arrows indicate the time point at which AMF is applied. b) Fluorescence microscopy images of DLD-1 colon cancer cells treated with Dox⊂SMNPs with (left) and without (right) the application of a 10 minutes continuous AMF (500 kHz, 37.4 kA m^{-1}). Images from top to bottom: Differential interference contrast (DIC) image showing the cell morphology. DAPI-stained image showing the nuclei (DAPI = 4′,6-diamidino-2-phenylindole). Dox fluorescence indicating the presence of Dox. Merged image of DAPI and Dox. Dox molecules are released from Dox⊂SMNPs upon AMF application and then enter into nuclei, which leads to cell apoptosis. Scale bar: 10 μm. c) Cell viability results of DLD-1 cells treated with and without Dox⊂SMNPs before and after application of AMF for 10 minutes through a CCK-8 assay (***$p \le 0.001$).

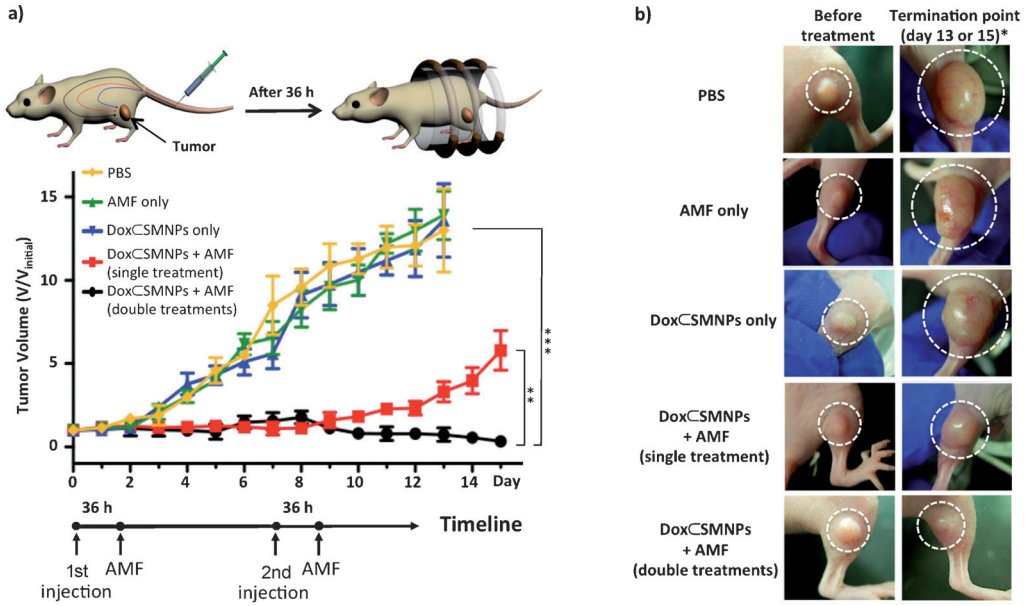

Figure 3. Evaluation of in vivo therapeutic efficacy. a) Treatment scheme of Dox⊂SMNPs in mouse and results of the tumor volume change over the course of the treatment (15 days) in DLD-1 xenografted mice ($n=3$) treated with Dox⊂SMNPs (w/and w/o application of AMF) and other controls (AMF only and PBS only). All injections were done on day 0 (and day 7 for the double injection group) when the tumor volume reached 100 mm^3; AMF application was performed at 36 h post-injection. The best tumor suppression result was observed in the group treated with a double injection of Dox⊂SMNPs with AMF application. The group treated with a single injection of Dox⊂SMNPs with AMF and the other control groups (i.e., treated with Dox⊂SMNPs only, AMF only and PBS only) show either a smaller degree or none of tumor suppression effects (**$p \leq 0.01$; ***$p \leq 0.001$). b) Tumor images of groups treated with Dox⊂SMNPs w/and w/o application of AMF and other controls, before treatment (left panels) and at the termination point (right panels). *The termination point of the experiment occurred either on day 15 or when the tumor volume reached 1500 mm^3.

injected Dox⊂SMNPs with AMF application. In addition, the drug-free vector (SMNPs w/o Dox) was administered following the same protocol, which gives similar results as control groups indicating that the effect of thermal heating by SMNPs is negligible (see the Supporting Information). It is notable that our Dox⊂SMNPs system only requires a low amount of drug (2.8 μg kg^{-1} Dox per injection) for tumor suppression, which is three orders of magnitude less than other NP systems (see Table S1 in the Supporting Information).[6d, 19]

In conclusion, we successfully demonstrate an on-demand drug delivery/release system that uses magnetothermally responsive Dox⊂SMNPs for highly effective in vivo cancer treatment. An optimized in vivo treatment protocol of Dox⊂SMNPs was designed after studying their biodistribution at a systemic level and evaluating in vitro the trigger release of Dox under optimal AMF condition. This on-demand drug release system used 1/1000 of the drug dosage compared to existing protocols (see the Supporting Information). We expect that this cutting edge drug delivery/release system with spatio-temporal controllability may open up clinical opportunities for drug candidates that exhibit good therapeutic efficacy but fail toxicology testing by ensuring increased selectivity and reducing side effects.

Received: September 25, 2012
Revised: February 19, 2013
Published online: March 20, 2013

Keywords: drug delivery · magnetic heat induction · magnetic nanoparticles · molecular imaging · supramolecular chemistry

[1] T. M. Allen, P. R. Cullis, *Science* **2004**, *303*, 1818–1822.
[2] a) M. E. Davis, Z. Chen, D. M. Shin, *Nat. Rev. Drug Discovery* **2008**, *7*, 771–782; b) R. A. Petros, J. M. DeSimone, *Nat. Rev. Drug Discovery* **2010**, *9*, 615–627; c) A. Z. Wang, R. Langer, O. C. Farokhzad, *Annu. Rev. Med.* **2012**, *63*, 185–198; d) C. Tassa, S. Y. Shaw, R. Weissleder, *Acc. Chem. Res.* **2011**, *44*, 842–852.
[3] V. Torchilin, *Adv. Drug Delivery Rev.* **2011**, *63*, 131–135.
[4] a) Y. Matsumura, H. Maeda, *Cancer Res.* **1986**, *46*, 6387–6392; b) S. Dufort, L. Sancey, J. L. Coll, *Adv. Drug Delivery Rev.* **2012**, *64*, 179–189.
[5] a) J. Ge, E. Neofytou, T. J. Cahill, R. E. Beygui, R. N. Zare, *ACS Nano* **2012**, *6*, 227–233; b) H. Yan, C. Teh, S. Sreejith, L. Zhu, A. Kwok, W. Fang, X. Ma, K. T. Nguyen, V. Korzh, Y. Zhao, *Angew. Chem.* **2012**, *124*, 8498–8502; *Angew. Chem. Int. Ed.* **2012**, *51*, 8373–8377.
[6] a) T. J. Harris, G. von Maltzahn, A. M. Derfus, E. Ruoslahti, S. N. Bhatia, *Angew. Chem.* **2006**, *118*, 3233–3237; *Angew. Chem. Int. Ed.* **2006**, *45*, 3161–3165; b) G. Wu, A. Mikhailovsky, H. A. Khant, C. Fu, W. Chiu, J. A. Zasadzinski, *J. Am. Chem. Soc.* **2008**, *130*, 8175–8177; c) A. Désert, I. Chaduc, S. Fouilloux, J. C. Taveau, O. Lambert, M. Lansalot, E. Bourgeat-Lami, A. Thill, O. Spalla, S. Ravaine, E. Duguet, *Polym. Chem.* **2012**, *3*, 1130–1132; d) A. Agarwal, M. A. Mackey, M. A. El-Sayed, R. V. Bellamkonda, *ACS Nano* **2011**, *5*, 4919–4926; e) P. Pradhan, J. Giri, F. Rieken, C. Koch, O. Mykhaylyk, M. Doblinger, R. Banerjee, D. Bahadur, C. Plank, *J. Controlled Release* **2010**, *142*, 108–121.

[7] H. Wang, S. T. Wang, H. Su, K. J. Chen, A. L. Armijo, W. Y. Lin, Y. J. Wang, J. Sun, K. Kamei, J. Czernin, C. G. Radu, H. R. Tseng, *Angew. Chem.* **2009**, *121*, 4408 – 4412; *Angew. Chem. Int. Ed.* **2009**, *48*, 4344 – 4348.

[8] K. J. Chen, S. M. Wolahan, H. Wang, C. H. Hsu, H. W. Chang, A. Durazo, L. P. Hwang, M. A. Garcia, Z. K. Jiang, L. Wu, Y. Y. Lin, H. R. Tseng, *Biomaterials* **2011**, *32*, 2160 – 2165.

[9] S. T. Wang, K. J. Chen, T. H. Wu, H. Wang, W. Y. Lin, M. Ohashi, P. Y. Chiou, H. R. Tseng, *Angew. Chem.* **2010**, *122*, 3865 – 3869; *Angew. Chem. Int. Ed.* **2010**, *49*, 3777 – 3781.

[10] a) H. Wang, K. J. Chen, S. T. Wang, M. Ohashi, K. I. Kamei, J. Sun, J. H. Ha, K. Liu, H. R. Tseng, *Chem. Commun.* **2010**, *46*, 1851 – 1853; b) H. Wang, K. Liu, K. J. Chen, Y. J. Lu, S. T. Wang, W. Y. Lin, F. Guo, K. I. Kamei, Y. C. Chen, M. Ohashi, M. W. Wang, M. A. Garcia, X. Z. Zhao, C. K. F. Shen, H. R. Tseng, *ACS Nano* **2010**, *4*, 6235 – 6243; c) K. Liu, H. Wang, K. J. Chen, F. Guo, W. Y. Lin, Y. C. Chen, D. L. Phung, H. R. Tseng, C. K. F. Shen, *Nanotechnology* **2010**, *21*, 445603-445610.

[11] Y. Liu, H. Wang, K. Kamei, M. Yan, K. J. Chen, Q. H. Yuan, L. Q. Shi, Y. F. Lu, H. R. Tseng, *Angew. Chem.* **2011**, *123*, 3114 – 3118; *Angew. Chem. Int. Ed.* **2011**, *50*, 3058 – 3062.

[12] K. J. Chen, L. Tang, M. A. Garcia, H. Wang, H. Lu, W. Y. Lin, S. Hou, Q. Yin, C. K. F. Shen, J. J. Cheng, H. R. Tseng, *Biomaterials* **2012**, *33*, 1162 – 1169.

[13] S. Acharya, S. K. Sahoo, *Adv. Drug Delivery Rev.* **2011**, *63*, 170 – 183.

[14] a) D. Yoo, J. H. Lee, T. H. Shin, J. Cheon, *Acc. Chem. Res.* **2011**, *44*, 863 – 874; b) J. H. Lee, J. T. Jang, J. S. Choi, S. H. Moon, S. H. Noh, J. W. Kim, J. G. Kim, I. S. Kim, K. I. Park, J. Cheon, *Nat. Nanotechnol.* **2011**, *6*, 418 – 422; c) S. H. Noh, W. Na, J. T. Jang, J. H. Lee, E. J. Lee, S. H. Moon, Y. Lim, J. S. Shin, J. Cheon, *Nano Lett.* **2012**, *12*, 3716 – 3721; d) C. R. Thomas, D. P. Ferris, J. H. Lee, E. Choi, M. H. Cho, E. S. Kim, J. F. Stoddart, J. S. Shin, J. Cheon, J. I. Zink, *J. Am. Chem. Soc.* **2010**, *132*, 10623 – 10625; e) J. T. Jang, H. Nah, J. H. Lee, S. H. Moon, M. G. Kim, J. Cheon, *Angew. Chem.* **2009**, *121*, 1260 – 1264; *Angew. Chem. Int. Ed.* **2009**, *48*, 1234 – 1238.

[15] H. Cabral, Y. Matsumoto, K. Mizuno, Q. Chen, M. Murakami, M. Kimura, Y. Terada, M. R. Kano, K. Miyazono, M. Uesaka, N. Nishiyama, K. Kataoka, *Nat. Nanotechnol.* **2011**, *6*, 815 – 823.

[16] a) C. Suckow, C. Kuntner, P. Chow, R. Silverman, A. Chatziioannou, D. Stout, *Mol. Imaging Biol.* **2009**, *11*, 100 – 106; b) D. Stout, A. Chatziioannou, T. Lawson, R. Silverman, S. Gambhir, M. Phelps, *Mol. Imaging Biol.* **2005**, *7*, 393 – 402; c) C. A. Boswell, X. K. Sun, W. J. Niu, G. R. Weisman, E. H. Wong, A. L. Rheingold, C. J. Anderson, *J. Med. Chem.* **2004**, *47*, 1465 – 1474.

[17] a) V. Y. Erukova, O. O. Krylova, Y. N. Antonenko, N. S. Melik-Nubarov, *Biochim. Biophys. Acta Biomembr.* **2000**, *1468*, 73 – 86; b) E. Hayakawa, K. Furuya, H. Ueno, T. Kuroda, M. Moriyama, A. Kondo, *Chem. Pharm. Bull.* **1991**, *39*, 1009 – 1012; c) M. K. Yu, Y. Y. Jeong, J. Park, S. Park, J. W. Kim, J. J. Min, K. Kim, S. Jon, *Angew. Chem.* **2008**, *120*, 5442 – 5445; *Angew. Chem. Int. Ed.* **2008**, *47*, 5362 – 5365.

[18] W. Zoli, P. Ulivi, A. Tesei, F. Fabbri, M. Rosetti, R. Maltoni, D. C. Giunchi, L. Ricotti, G. Brigliadori, I. Vannini, D. Amadori, *Breast Cancer Res.* **2005**, *7*, R681 – R689.

[19] a) W. Zhang, Z. Y. Guo, D. Q. Huang, Z. M. Liu, X. Guo, H. Q. Zhong, *Biomaterials* **2011**, *32*, 8555 – 8561; b) Z. Liu, A. C. Fan, K. Rakhra, S. Sherlock, A. Goodwin, X. Y. Chen, Q. W. Yang, D. W. Felsher, H. J. Dai, *Angew. Chem.* **2009**, *121*, 7804 – 7808; *Angew. Chem. Int. Ed.* **2009**, *48*, 7668 – 7672.

